DOI: http://dx.doi.org/10.1016/j.indcrop.2013.06.033

Effect of fibre configurations on mechanical properties of flax/tannin composites

J Zhu[a], J Njuguna[a,f,*], H Abhyankar[a], H Zhu[b], D Perreux[c], F Thiebaud[c], D Chapelle[c], A Pizzi[d,e], A Sauget[d], D L Alain[d] and A Nicollin[d]

[a] Centre of Automotive Technology, Cranfield University, Cranfield, Bedfordshire, MK43 0AL, UK

[b] Cranfield Health, Cranfield University, Cranfield, Bedfordshire, MK43 0AL, UK

[c] MAHYTEC, 210 avenue de Verdun, 39100 Dole, France

[d] LERMAB-ENSTIB, University of Lorraine, 88051 EPINAL cedex 9, Epinal, France

[e]King Abdulaziz University, Jeddah, Saudi Arabia

[f]Institute for Innovation, Design and Sustainability, Robert Gordon University, Aberdeen, AB25 1HG, UK

* Corresponding author: J Njuguna (E: j.njuguna@cranfield.ac.uk, T: +44 (0)1234 754186)

Key words: Laminate, Flax fibre, Biocomposite, Tannin, Compression moulding

Abstract.

Flax reinforced tannin-based composites have a potential to be used in vehicle applications due to the environmental advantages and good mechanical properties. In this paper, the effects of fibre configuration on mechanical properties of flax/tannin composites were investigated for nonwoven and woven fabric lay-up angles (UD, $[0°, 90°]_2$ and $[0°, +45°, 90°, -45°]_2$). The tannin/flax composites were prepared by compression moulding. The manufactured specimens were then characterized for quasi-static tensile properties, dynamic mechanical properties and low-energy impact performance. Failure mechanism was further investigated using microscopy and demonstrated the need for further adhesion improvements. The study shows that the UD fabric reinforced composite performs better in tensile strength and modulus whereas $[0°, +45°, 90°, -45°]_2$ composite provides the best impact energy absorption performance.

1 Introduction

Natural fibre-reinforced composites have attracted the interest of many industries (Kalia et al., 2011) due to their comparative mechanical properties and outstanding bio-degradability characteristics. Natural fibres are known to be bio-degradable, CO_2 neutral (remove carbon dioxide from the atmosphere), low density/price and non-toxic, compared to the established synthetic fibres (Bos, 2004; Fan et al., 2011).

Flax fibres like other lingnocellulosic fibres are inexpensive, have good recyclability, and are widely investigated for manufacturing composites.

In the area of flax fibre reinforced composites, most of the research (Bos et al., 2006; Van de Velde and Kiekens, 2001; Van Den Oever et al., 2000; Åkesson et al., 2011) focuses on Polypropylene (PP)-based, epoxy-based (synthetic and natural) and Polylactic acid (PLA)-based composites. Polypropylene (PP) is the most common synthetic thermoplastic matrix for flax fibre reinforcement on account of its low density, low thermal expansion, good resistance to water and recyclability. Garkhail, Heijenrath and Peijs (Garkhail et al., 2000) used maletic-anhydride grafted PP (MA-PP) to prepare the flax composites through two processing methods: film-stacking and paper-making process. The effects of alignment structure of flax fibres in PP based composite was addressed by Van Den Oever, Bos and Van Kemenade (Van Den Oever et al., 2000). Synthetic thermosets including epoxy, phenolic etc.are also used for the preparation of flax composites. For example, the tensile deformation behaviour of polyester resin/flax thermoset composites was studied by Hughes et al. (Hughes et al., 2007). In addition to the synthetic polymer matrices, the use of bio-polymers as matrix materials has been increasing rapidly in the recent years. Saiah and his co-workers (Saiah et al., 2009) reinforced the thermoplastic derived from wheat flour by flax fibres and used X-ray diffraction to analyse the crystallinity of the fibres. The increase in fibre content led to the increase in intensity of peaks at 2θ of 15.1°, 16.8°, 22.7° and 34.4°, corresponding to crystalline structure of flax fibres. Adhekunle et al. (Adekunle et al., 2012) manufactured flax/bio-thermoset (methacrylated soybean oil and methyacrylic anhydride modified soybean oil) composites with different fibre stacking sequences and lay-up angles, leading to the maximum tensile strength of 119 MPa and Young's modulus of 14 GPa. Akesson et al. (Åkesson et al., 2011) fabricated the flax-reinforced PLA composite, which was cured at elevated temperature via compression moulding. They performed DMA analysis and found that the storage modulus of PLA composites reinforced with 70 wt% flax fibres is 9.32 GPa and 3.29 GPa at 20 °C and 140 °C, respectively. **Table 1** exhibits some mechanical properties of selected flax reinforced polymer composites through recent research.

One possible matrix for fully bio-degradable flax composites is tannin resins (bio-resins) from plant sources (e.g. wattle, myrtle, pine etc.). Tannins contain many phenolic rings and have a high molecular range of 500 to 2000 and are chemically grouped into hydrolysable and condensed tannin. The hydrolysable tannin is capable of hydrolysing in certain conditions (e.g. alkalis, acids and enzymes),

whereas the condensed tannin is more stable and suitable to produce resins (Pizzi and Mittal, 2003). Tannin crosslinking by formaldehyde via methylene or methylene ether bridges in a polycondensation reaction is the traditional chemisry for tannins to function as exterior-grade weather-resistant wood adhesives (Pizzi, 1983; Pizzi, 1994; Pizzi and Mittal, 2003). To decrease or completely eliminate formaldehyde emission during processing, the use of hexamethylenetetramine (hexamine) was developed as an effective alternative to traditional hardeners (**Figure 1**). Compared to the widely reported tannins for adhesive applications (Bisanda et al., 2003), there are only a small number of papers about tannin matrix composites. Coir fibre reinforced tannin composites were recently studied by Vilmar et al. (Barbosa Jr. et al., 2010) for potential use in automotive applications as internal parts. Ndazi and his co-workers (Ndazi et al., 2006) manufactured composite panel boards from rice husks and mimosa tannin resins. The use of tannin matrix has garnered attention for the following reasons: (i) non-toxic nature of tannin and related hardeners; (ii) wide availability of tannin and resulted cheaper cost; (iii) fast curing rate of tannin resins. The environmental and economic benefits of tannin composites have attracted lots of attention from auto industry. The composite made from tannin and flax fibres could potentially offer desirable characteristics aiming at reducing the environmental footprint of superlight electric vehicles through the use of bio-materials for load-bearing parts such as vehicle body panels, crash elements, side panels and body trims (Fan et al., 2011; Zhu et al, 2012).

Whole bioresin/flax fibre-reinforced composites suitable for structural applications (e.g. in load bearing automotive parts) are yet to be realised. On-going research to improve the resin—natural fibres interface remains the key challenge and as a result, the flax/tannin composites publications are rare in the open literature. An important study on the non-woven flax mats as reinforcement in flax/tannin composites was conducted by Pizzi et al. (Pizzi et al., 2009) who reported 50% increase of tensile strength from 536 to727 Kg/m^3. They studied two tannin resins formulations: (1) mimosa tannin with 5% hexamine as hardener; and (2) mixed tannin/lignin resins in 50/50 solid content. The fibre configuration which plays a significant part in mechanical properties for these composites is not investigated in the literature and such works are yet to be reported in the open literature.

Therefore, our work builds up on our earlier studies (Pizzi et al., 2009; Fan et al., 2011; Zhu et al, 2012) by focusing on the effects of fibre configurations on mechanical properties of flax/tannin composites. The temperature dependency of mechanical properties was indicated through DMA

characterisation. Tensile properties including the values and the failure mechanisms were obtained using the DIC (digital image correlation) tensile measurement, followed by the SEM (Scanning electronic micrograph) on the failed samples. The drop weight impact tests were also performed to show the dynamic impact resistance, which plays an important role for automotive structural parts.

2 Materials and methods

2.1 Materials

Non-woven flax mats (areal weight 1200 g/mm^2, thickness 5mm) were provided by CETELOR, Epinal, France and were un-treated chemically. The unidirectional fabrics (areal weight 180 g/mm^2, thickness 0.35 mm) provided by LINEO were pre-coated for epoxy impregnation. Mimosa tannin resin was supplied by Silva Chimica, S. Michele Mondovi, Italy. As shown in **Table 2**, the non-woven flax mat/tannin composites were denoted as type A, while woven fabric-reinforced laminate composites were manufactured as type B, C and D with different lay-up angles (See in **igure 2**). All the laminates had the fibre content of around 50% in weight and a target thickness of 3 mm, and specimen was machined into the required sizes for tests and characterisations.

2.2 Preparation of composites

Compression moulding process was used to produce all of the tannin-based laminate composites. Proper drying of flax fibres was carried out prior to the fabrication to avoid poor adhesion between fibres and matrix. The composite plates were fabricated using a 100t hydraulic press with servo-component allowing an accurate control of the consolidation pressure. The pressing blocks of the press were surrounded by an electric furnace with multi-segments controller for programming polymerization cycle. Additionally, a small-diameter thermocouple was placed in the mould in order to measure temperature accurately. To reduce the thermal inertia of the mould for the optimization of curing and consolidation cycle, a thin-walled aluminium mould was used. Quality and repeatability requirements imposed to systematically respect a strict fabrication protocol from the mould preparation.

2.3 Characterisation and mechanical testing

Dynamic mechanical thermal analysis

Dynamic mechanical analysis was conducted in a Thermal Analysis Instruments Q800 DMA using single cantilever bending mode and liquid nitrogen cooling system. The temperature range was from room

temperature to 250°C at a heating rate of 3°C/min and a frequency of 1 Hz. One specimen was tested for every composite type and the testing surface area was about 35mm ×12 mm. The effect of temperature on mechanical parameters (e. g storage modulus, loss modulus and tanδ) was analysed from the obtained results.

Scanning electron microscope

The cross-section surface topographies of the composites after tensile testing were examined using a XL30 SFEG analytical high resolution scanning electron microscope (SEM), supplied by FEI. Prior to SEM investigation, the test specimens were vacuum –coated with thin layers of gold powder to avoid the electrical charging during analysis. The whole examination was carried out at 5V and room temperature to produce micrographs of surfaces at various magnifications.

Quasi-static tensile tests

The flat coupon tensile test was carried out on the Instron 50/100 kN machine according to ASTM D3039 at the cross head speed of 2mm/min. The test specimens were cut at the standard size of 250mm ×25mm and an average thickness of 2.5 mm. To obtain micro-scale elongation information for accurate surface strain, digital image correlation (DIC) system was applied during the tensile tests of each specimen (see **Figure 3**).

Low-energy impact tests

Impact strength is greatly influenced by various factors, such as the fibre architecture and matrix/fibre adhesions. The drop-tower tests were performed using an Instrumented Falling Weight Impact Tester, Type 5, according to ASTM D7136, to provide the impact information like maximum force and impact energy. Through Newton's law, the total input energy was determined by the impactor mass and the nominal impact velocity of 3m/s. 100mm ×150mm specimens (regular plaques) with average thickness of 2.5mm were tested.

3 Results and discussion

3.1 Effect of fibre configurations on DMA results

Dynamic mechanical analysis was carried out to study the effect of temperature on the viscoelastic properties of tannin/flax composites. Three important parameters—storage modulus (E'), loss modulus

(E'') and tan δ (the ratio of E''/E'), were obtained over the temperature range from room temperature to 250°C. The recorded viscoelastic data are plotted as **Figure 4**, **Figure 5** and **Figure 6** on the basis of each parameter, and **Table 3** summarizes the transition temperatures and other characteristic properties. The DMA analysis could be further clarified with neat cured tannin resins, however to date, the author has not managed to cure tannin resins without fibres. This can also be clarified by the complete lack of literature on DMA properties of cured neat tannin resins, except for cured neat tannin adhesives (Vázquez et al., 2012), the results of which are not comparable to the resins used for the study.

The storage modulus of unwoven flax mat reinforced composite (type A) at 27°C was 5.4 GPa, displaying a fairly good correlation with results (Young's modulus of 6.4 GPa) obtained from tensile tests (see in following chapter 3.2). In terms of the woven flax/tannin composites (type B, C and D), the initial storage modulus follow the trend B>C>D. The UD (0°) composite (type B) showed the highest the modulus (7.5 GPa) attributable to reinforce angle of 0°. The storage modulus decreases with increasing the fibre orientation from 0° to 90° according to the equation (De and White, 1996).

$$1/E_c' = cos^2\theta/E_L' + sin^2\theta/E_T' \quad (1)$$

Where θ is the fibre orientation, E' is the storage modulus of composites, E_L' is the modulus along the direction of the fibre alignment, E_T' is the transvers modulus. The highest storage modulus is reached at the longitudinal direction (θ=0°). The used fibre fabrics in flax/tannin composites could be assumed as one-directional reinforcement. The composite $[0, 90°]_4$ (type C) had a higher storage modulus at 27°C than the composite $[0, +45°, 90°, -45°]_2$ (type D) due to the fact that type C contains more UD-aligned fibre fabrics. The initial storage modulus of the composite $[0, +45°, 90°, -45°]_2$ (type D) (27°C) was observed almost to be the same as the one of the nonwoven flax/tannin composite (type A). This indicates that the fabric lay-up structure of $[0, +45°, 90°.-45°]_2$ shows similar effects on mechanical properties to the nonwoven flax mat (2 plies) at room temperature.

Figure 4 shows the temperature dependency of the storage modulus (E') on various composite samples. The storage modulus of non-woven flax mat/tannin composite (type A) dropped from 5.3 GPa at 27°C to 636 MPa at 200°C with a transition around 150°C, related to the possible degradation. A similar transition temperature of 160°C was observed for composites B, C and D. The slight transition change at around 50°C reflect the progressive glass/rubber transition of the composites. The onset of the glass transition was observed from storage modulus spectrum.

The variation in loss modulus of the flax/tannin composites is shown in Figure 5. It has been reported that it is more reliable to obtain glass transition temperature (Tg) from the peak of loss modulus than from the tan δ peak which tends to overestimate T_g (Adekunle et al., 2012). The T_g of composites type A, C and D on average was about 60.5°C, whereas a broad and fuzzy T_g peak at around 50°C was observed for type B (UD type). More constraints on molecule motion with increasing the fibre angle (θ) may be the reason for the increase of T_g (Seyler, 1994). In addition, the composite type B has more UD fibre fabrics as reinforcement at 0°, thus the resin matrix at the fibre surface is stiffer and deformed less than the absorbed resin layer in other composite systems. Consequently, the larger gradients in elastic modulus of tannin resins cause a broader glass transition range.

Figure 6 shows variation of tanδ as a function of temperature. The tanδ trend is indicative of energy dissipation with regards to the changes in the physical properties. Clearly, there were three tanδ peaks observed in the curve of the composite $[0, +45°, 90°, -45°]_2$ (type D). The first peak with increasing temperature expressed as T_g at around 65°C, slightly higher than that obtained from loss modulus-temperature curve. The second peak, called β transition, may be attributed to the water evaporation phenomenon or due to the motion of side groups grafted on molecular chains on account of the absorbed kinetic energy. The third peak close to 200°C probably arises from the onset of degradation of flax fibres, affecting the fibre load-carrying ability and hence the properties of the attached reins. This shows agreement with the published fibre degradation temperature (Summerscales et al., 2010).

3.2 Effect of fibre configuration on tensile properties

Both macro and micro-scale tensile data was obtained through the DIC-tensile experiments. Tensile strength, maximum strain, tensile modulus were easily read from the micro-scale stress-strain curves. The macro-scale load-elongation curves after the maximum load were used to reflect the macro failure mechanism.

Using DIC to reduce the factor of dimension change under stress, Figure 7 shows the relationship between stress and strain of tested composites at micro-scale level. Since the stress-strain curves measured by DIC were theoretically non-linear, the quantitative values were plotted as scatter diagrams. UD (0°) samples (type B) had the highest tensile strength of up to 140 MPa, which is in line with the reported value (150MPa) of the dobby weaved flax/bio-thermoset composite (Adekunle et al., 2012; Åkesson et al., 2011). The [0, +45°, 90°,-45°]2 composite with lower tensile strength but higher

maximum strain was found to be tougher than the [0, 90°]4 type. The tensile strength and maximum strain of nonwoven flax mat/mimosa tannin composites (type A) reached relatively low values of 55 MPa and 0.7%, respectively, due to the random distribution of short flax fibres in non-woven fibre mats.

Figure 8 represents the tensile modulus for each composite type. Young's modulus was measured as the tangent modulus in the initial linear portion in the curves. The Young's modulus of woven fabric reinforced specimens follows the trend B>C>D. The unidirectional fibres in type B apparently give rise to the maximum Young's modulus of approximately 9.6 GPa. In accordance with the tensile strength, the $[0, 90°]_4$ layer arrangement (type C) produced higher Young's modulus of 4.8 GPa than the $[0, 45°, 90°, -45°]_2$ composite (type D). It was observed that that the non-woven flax mat reinforced tannin composites (type B) also showed a relatively high Young's modulus (6.4 GPa). Due to the different manufacturing methods, tensile modulus of type A is not comparable to types (B, C and D).

It can be seen from **Figure 9** that fabric layers of composite B after testing were separated, compared to tensile fractured composite A. **Figure 10** shows the load-extension curves for the tannin composites. Unlike the three composite types (B, C and D), after the maximum force, the loads applied on the flax mat composite (type A) decreased immediately (z-curves in **Figure 10**). The first peak of composite B may be due to the combination of failure of tannin resins and the first delamination. However, it is very likely that the progress of specimen delamination is not in a continuous and smooth fashion but rather in an abrupt and irregular way. The load went to high levels before the sudden debonding, at which the force subsequently dropped down. This delamination behaviour indicates that the tannin resin did not fully wet within the eight fibre plies. Another reason for the delamination is the low fibre/matrix interface strength, as a result of the incompatibility between hydrophilic flax fibres and hydrophobic tannin resins.

To further understand the tensile failure mechanisms, SEM micrographs for tensile surfaces of flax/tannin composites are shown in Figure 11 and Figure 12. Bax and Müssig (Bax and Müssig, 2008; Hughes et al., 2007) used SEM to characterise the failure mechanisms of natural composites. As discussed previously, composites B, C and D showed delamination behaviour without fracture during tensile testing. The delaminated sample was then cut and investigated under SEM. Figure 11 (a) shows the separation of fibre layers upon testing. It indicates the poor wettability between these fabric layers. Some noticeable gaps between matrix and fibres are indicated by 'A' in **Figure 11** (b). These empty gaps indicate the poor interface contact between fibres and can also account for the weak load transfer and

unexpected performance. To improve the compatibility, fibre surface treatment like alkali treatment was used by Yan et al. (Yan et al., 2012).

Figure 12 is the cross-sectional micrographs of tensile fracture surface. The failure mechanism shown in the figure is complicated. From **Figure 12** (a), the bonding quality between fibre layers is better than that of non-fracture specimens. **Figure 12** (b) shows the remaining holes (indicated by 'B') possibly after fibre pull-out. The fibre breakage shown in **Figure 12** (c) is caused by the applied stress. Symbol 'C' in **Figure 12 (**d)) points to a small crack within the tannin resins adjacent to fibres. This crack may be initiated at the end of failure and did not continue to propagate without enough energy. According to the above investigations, the failure of flax/ tannin composites is governed by the combination of fibre pull-out, fibre fracture and brittle fracture of tannin resins.

3.3 Effect of fibre configuration on impact properties

The basic impact behaviour of the flax fibre tannin matrix composites was analysed from **Figure 13** showing force versus vertical impactor displacement curves for different composite systems. Apparently, the composite A displayed classic behaviour of perforation, in which there was a continuous monotonic increment of z displacement with constant force. The other evidence is the (damage) image of sample A with a hole after impact (**Figure 14** (a)). At the perforation instant, the energy dissipation by system was switched from 'internal' fragmentation to friction between the dart surface and the perforation hole. As a result, the velocity decreased linearly with increasing dart displacement after perforation point at 15.3mm displacement (**Figure 15** plotted directly from the recorded impact data). The force also dramatically dropped to 186.8N at this moment and maintained the value for a period. In addition, the UD (0°) composite (type B) showed a similar impact performance to the nonwoven flax composite (type A). However, the perforation point was difficult to read from the irregular speed-displacement curve in **Figure 15**. The reason may be associated to the different failure mechanism during impact. For composite B, a crack propagated through the whole sample (**Figure 14** (b)) and broke it into two pieces. This is due to the horizontal weak interfacial phase in UD (0°) composites (composite B). Crack was initiated and then the weak transvers phases allowed crack propagation along the longitudinal direction. For type C, the dart stopped without rebounding while reaching the maximum penetration displacement of 18.7mm as seen in **Figure 13**. This can be interpreted asthe energy being completely dissipated by the specimen. There was no exchange residual energy with dart due to lack of rebound for composite C. It is noted that

the end curve of composite D folds towards decreasing displacement, which is a strong evidence of rebound. The amount of elastic energy stored by the specimen was released from the 'fold' point to the end and no further energy dissipation occurred. The fibre fabric layup of $[0, +45°, 90°, -45°]_4$ offered good stress transfer and even mechanical properties in various directions. As a conclusion, this fabric arrangement showed the best impact resistance implied by the presence of rebound (energy release).

The load-displacement curves (**Figure 16**) show the maximum force of the composites. The maximum force is generally marked as the occurrence of the first failure of laminates (Belingardi and Vadori, 2002). The composite $[0, +45°, 90°, -45°]_4$ (type D) had the highest maximum force of 1123N. From the point of view of the fibre direction distribution, the random fibre reinforced composite (type A) also enhanced the impact resistance more than the UD (0°) composite (type B) and the composite $[0, 90°]_4$ (type C). The trend of impact energy of test specimens is: C>D>A>B, as seen in **Figure 17**. The composites A and B exhibited much lower impact energy (6.9 and 6.8J, respectively) than the composites C and D since the specimens A and B were carried out in the perforation case. For composite A and B, a certain amount of energy was dissipated by friction, but not absorbed by samples. On the contrary, most of the energy was absorbed by composites C and D to stop the impactor. The impact energy of type D (10.6J) was slightly lower than the one of type C (10.8J). This slight difference is accredited to the energy released back to rebound dart during the impact tests of composite D.

4 Conclusions

The effect of fibre configuration on mechanical performance of flax/tannin composites was investigated. The UD (0°) composites (type B) showed the highest tensile strength of up to 140 MPa and elastic modulus of 9.6 MPa, as a result of the longitudinal reinforcement in the testing direction. The initial storage modulus of the composites shows strong agreement with the tensile properties. The glass transition temperature of composites was around 60°C. It was found that failure mechanisms of the tensile fractured samples include fibre pull-out, fibre breakage and brittle tannin failure. In addition, the nonwoven flax mat/tannin composite (type A) and the $[0, +45°, 90°, -45°]_4$ composite (type D) displayed the good impact performance due to the even distribution of stiffness and strength in all directions. As for the fabric configurations, the investigations suggest that the fabric arrangement could be properly tailored to balance tensile properties and impact resistance. Also, with further surface treatment (e.g. alkali

treatment) to improve fibre/matrix adhesion, flax/tannin composite will possibly show improved mechanical properties including tensile strength.

Acknowledgement

The authors are thankful for the financial support by the European Commission Framework 7 through the ECOSHELL Project Reference No. 265838 entitled **'**Development of new light high-performance environmentally benign composites made of bio-materials and bio-resins for electric car application'. The authors would also like to acknowledge technical support at Cranfield University.

References

Adekunle, K., Cho, S., Ketzscher, R., Skrifvars, M., 2012. Mechanical properties of natural fiber hybrid composites based on renewable thermoset resins derived from soybean oil, for use in technical applications, J Appl Polym Sci 124, 4530-4541.

Adekunle, K., Cho, S.-, Patzelt, C., Blomfeldt, T., Skrifvars, M., 2011. Impact and flexural properties of flax fabrics and Lyocell fiber-reinforced bio-based thermoset, J Reinf Plast Compos 30, 685-697.

Åkesson, D., Skrifvars, M., Seppälä, J., Turunen, M., 2011. Thermoset lactic acid-based resin as a matrix for flax fibers, J Appl Polym Sci 119, 3004-3009.

Barbosa Jr., V., Ramires, E.C., Razera, I.A.T., Frollini, E., 2010. Biobased composites from tannin–phenolic polymers reinforced with coir fibers, Industrial Crops and Products 32, 305-312. doi: 10.1016/j.indcrop.2010.05.007.

Bax, B., Müssig, J., 2008. Impact and tensile properties of PLA/Cordenka and PLA/flax composites, Composites Sci. Technol. 68, 1601-1607. doi: 10.1016/j.compscitech.2008.01.004.

Belingardi, G., Vadori, R., 2002. Low velocity impact tests of laminate glass-fiber-epoxy matrix composite material plates, Int. J. Impact Eng. 27, 213-229.

Bisanda, E.T.N., Ogola, W.O., Tesha, J.V., 2003. Characterisation of tannin resin blends for particle board applications, Cement and Concrete Composites 25, 593-598.

Bos, H.L., 2004. The potential of Flax Fibre as Reinforcement for composite Materials, Technische Universiteit Eindhoven, ISBN 90-386-3005-0.

Bos, H.L., Müssig, J., van den Oever, M.J.A., 2006. Mechanical properties of short-flax-fibre reinforced compounds, Composites Part A: Applied Science and Manufacturing 37, 1591-1604.

De, S.K., White, J.R., 1996. Short Fibre-Polymer Composites. Woodhead, Cambridge.

Fan, J., Nassiopoulos, E., Brighton, J., De Larminat, A., Njuguna, J., 2011. New structural biocomposites for car applications, Society of Plastics Engineers - EUROTEC 2011 Conference Proceedings, Code 88784, 5 pages.

Garkhail, S.K., Heijenrath, R.W.H., Peijs, T., 2000. Mechanical properties of natural-fibre-mat-reinforced thermoplastics based on flax fibres and polypropylene, Applied Composite Materials 7, 351-372.

Hughes, M., Carpenter, J., Hill, C., 2007. Deformation and fracture behaviour of flax fibre reinforced thermosetting polymer matrix composites, J. Mater. Sci. 42, 2499-2511.

Kalia, S., Dufresne, A., Cherian, B.M., Kaith, B.S., Avérous, L., Njuguna, J., Nassiopoulos, E., 2011. Cellulose-Based Bio- and Nanocomposites: A Review, International Journal of Polymer Science, 2011, Article ID 837875, 35 pages, doi:10.1155/2011/837875

Muralidhar, B.A., Giridev, V.R., Raghunathan, K., 2012. Flexural and impact properties of flax woven, knitted and sequentially stacked knitted/woven preform reinforced epoxy composites, J Reinf Plast Compos 31, 379-388.

Ndazi, B., Tesha, J.V., Karlsson, S., Bisanda, E.T.N., 2006. Production of rice husks composites with Acacia mimosa tannin-based resin, J. Mater. Sci. 41, 6978-6983.

Oksman, K., 2001. High quality flax fibre composites manufactured by the resin transfer moulding process, J Reinf Plast Compos 20, 621-627.

Pichelin, F., Kamoun, C., Pizzi, A., 1999. Hexamine hardener behaviour: Effects on wood glueing, tannin and other wood adhesives, Holz als Roh - und Werkstoff 57, 305-307.

Pizzi, A., 1994. Advanced Wood Adhesives Technology. Dekker, New York.

Pizzi, A., 1983. Wood Adhesives : Chemistry and Technology. Dekker, New York.

Pizzi, A., Kueny, R., Lecoanet, F., Massetau, B., Carpentier, D., Krebs, A., Loiseau, F., Molina, S., Ragoubi, M., 2009. High resin content natural matrix-natural fibre biocomposites, Industrial Crops and Products 30, 235-240.

Pizzi, A., Mittal, K.L., 2003. Handbook of Adhesive Technology, 2nd ed. Marcel Dekker, New York.

Saiah, R., Sreekumar, P.A., Gopalakrishnan, P., Leblanc, N., Gattin, R., Saiter, J.M., 2009. Fabrication and characterization of 100% green composite: Thermoplastic based on wheat flour reinforced by flax fibers, Polymer Composites 30, 1595-1600.

Seyler, R.J., 1994. Assignment of the Glass Transition.

Summerscales, J., Dissanayake, N.P.J., Virk, A.S., Hall, W., 2010. A review of bast fibres and their composites. Part 1 - Fibres as reinforcements, Composites Part A: Applied Science and Manufacturing 41, 1329-1335.

Van de Velde, K., Kiekens, P., 2001. Thermoplastic polymers: overview of several properties and their consequences in flax fibre reinforced composites, Polym. Test. 20, 885-893. doi: 10.1016/S0142-9418(01)00017-4.

Van Den Oever, M.J.A., Bos, H.L., Van Kemenade, M.J.J.M., 2000. Influence of the physical structure of flax fibres on the mechanical properties of flax fibre reinforced polypropylene composites, Applied Composite Materials 7, 387-402.

Vázquez, G., Santos, J., Freire, M.S., Antorrena, G., González-Álvarez, J., 2012. DSC and DMA study of chestnut shell tannins for their application as wood adhesives without formaldehyde emission, Journal of Thermal Analysis and Calorimetry , 1-7.

Yan, L., Chouw, N., Yuan, X., 2012. Improving the mechanical properties of natural fibre fabric reinforced epoxy composites by alkali treatment, J Reinf Plast Compos 31, 425-437.

Zhu, J., Abhyankar, H., Nassiopoulos, E., Njuguna, J. 2012. Tannin-based flax fibre reinforced composites for structural applications in vehicles, IOP Conference Series: Materials Science and Engineering, 40 (1), 012030.

Figures

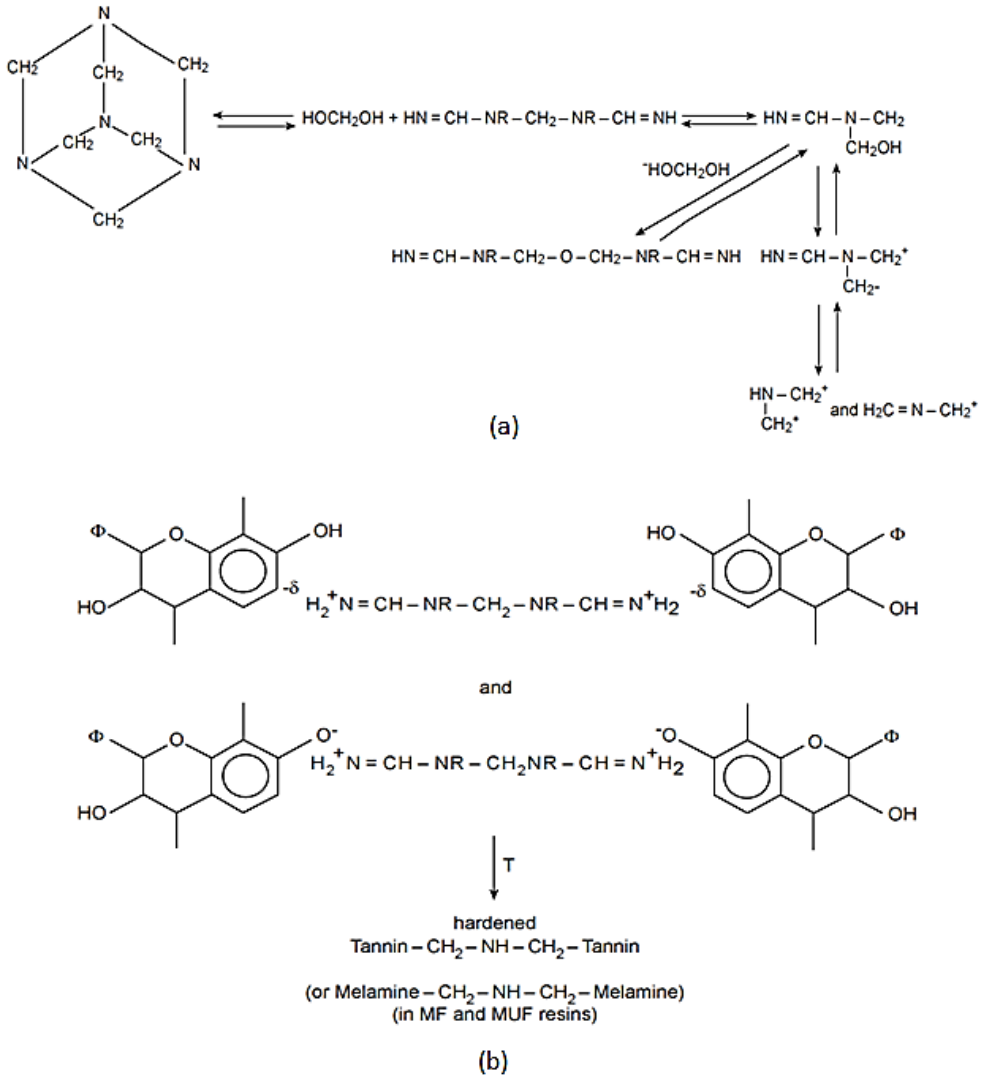

Figure 1. The chemical reaction between tannin and hexamine: (a) decomposition of hexamine; (b) polycondensation of condensed tannin (Pichelin et al., 1999).

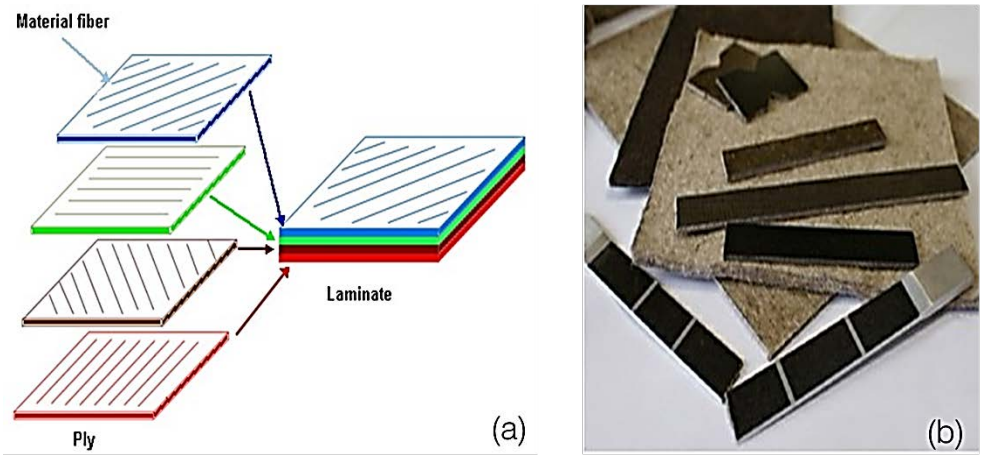

Figure 2. (a) The vary of lay-up angles in the laminate; (b) resulted bio-composites.

Figure 3. DIC technique applied to provide micro-scale information**.**

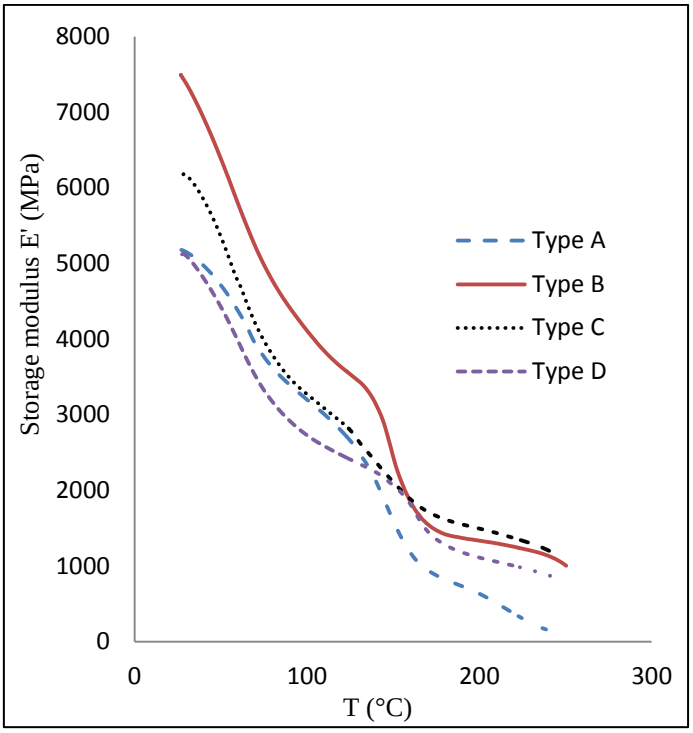

Figure 4. Variation of storage modulus of the flax/tannin composites

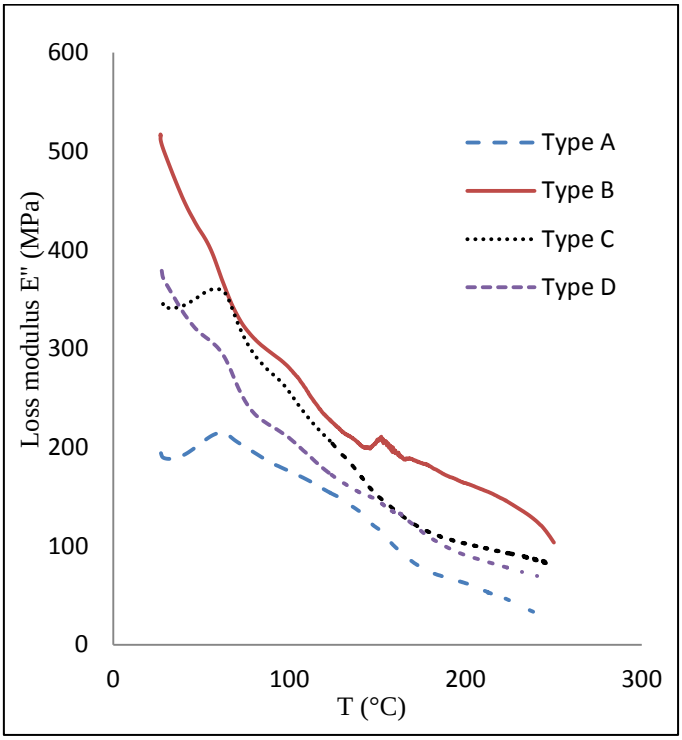

Figure 5. Variation of loss modulus (E'') of flax/tannin composites.

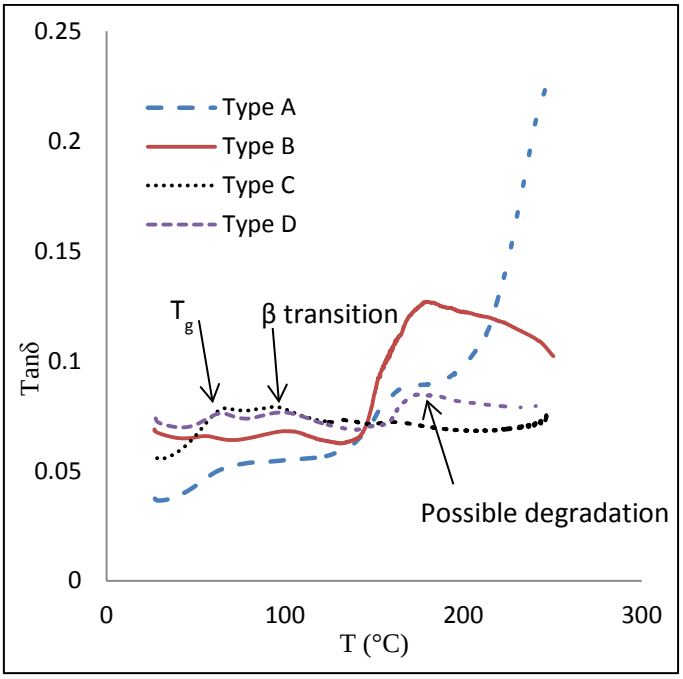

Figure 6. Variation of tanδ of flax/tannin composites.

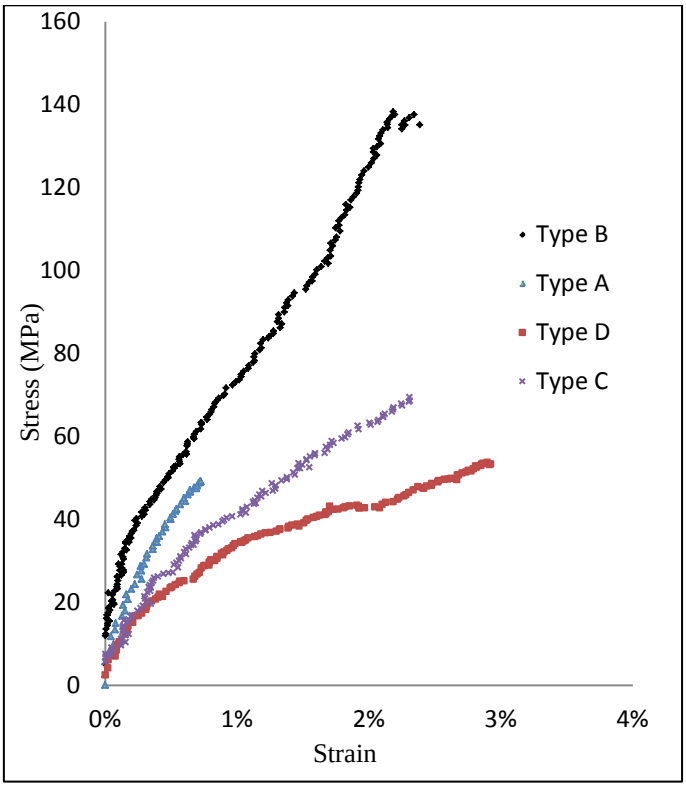

Figure 7. Micro-scale stress-strain curves obtained through DIC method.

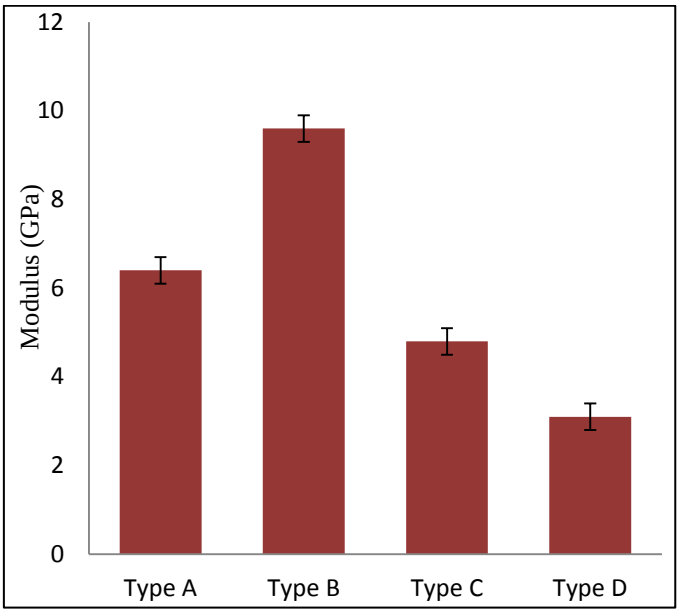

Figure 8. Tensile modulus of various flax/tannin composites.

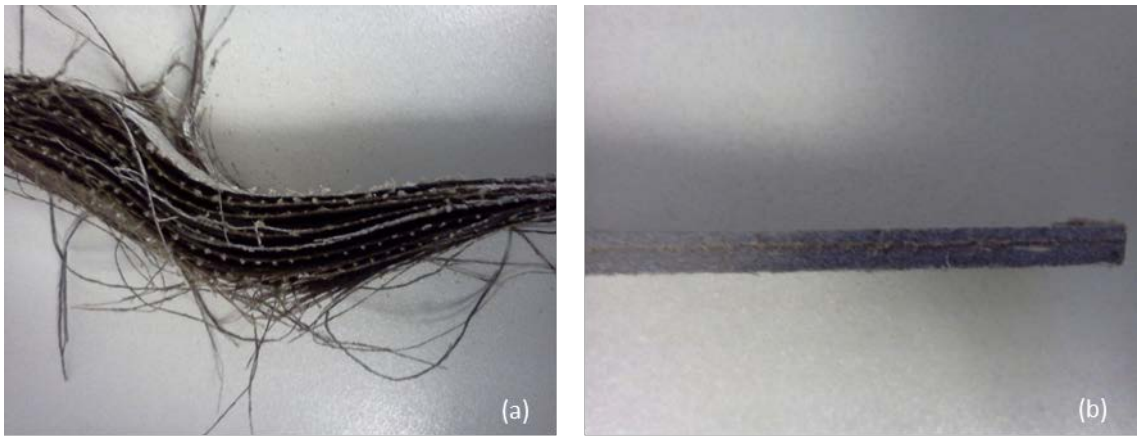

Figure 9. Failed samples during tension (a) delamination; (b) fracture.

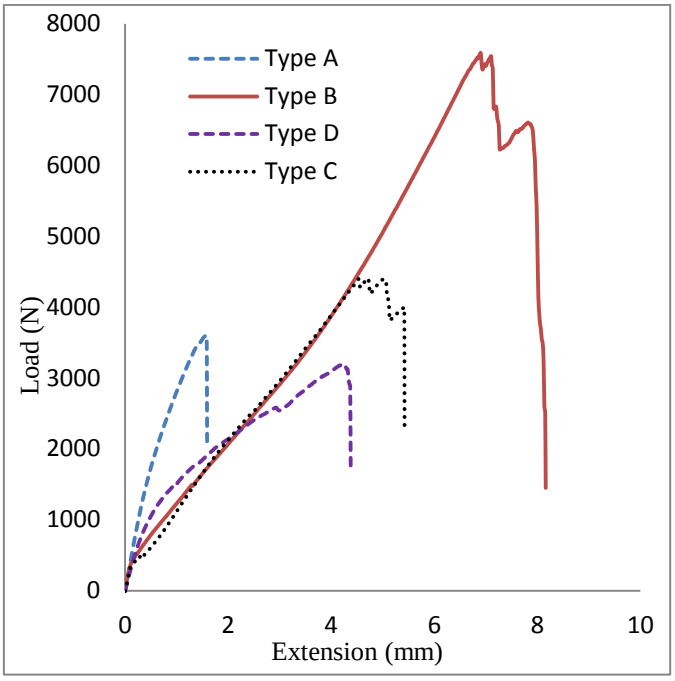

Figure 10. Load-elongation curves (macro-scale).

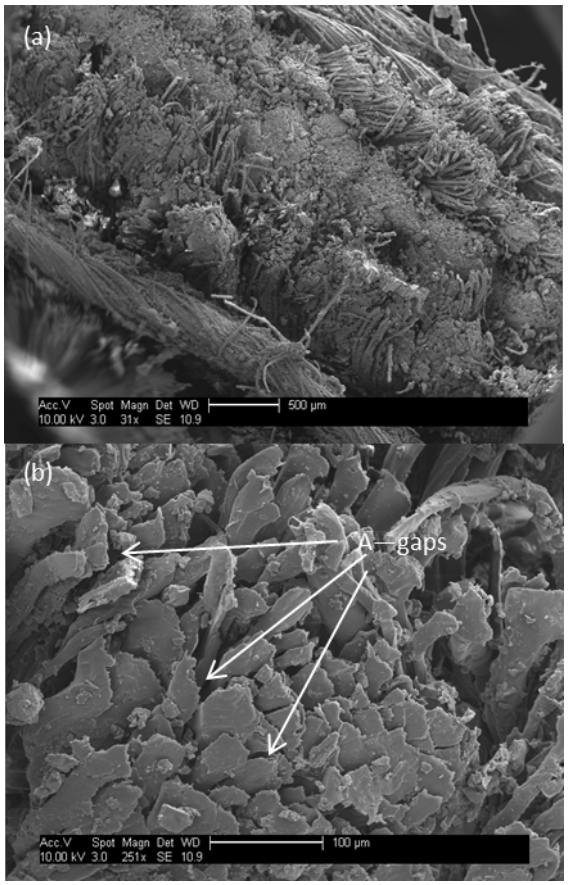

Figure 11. SEM micrographs of a cut non-fractured sample: (a) cross-section of the delaminated sample, (b) magnified graph.

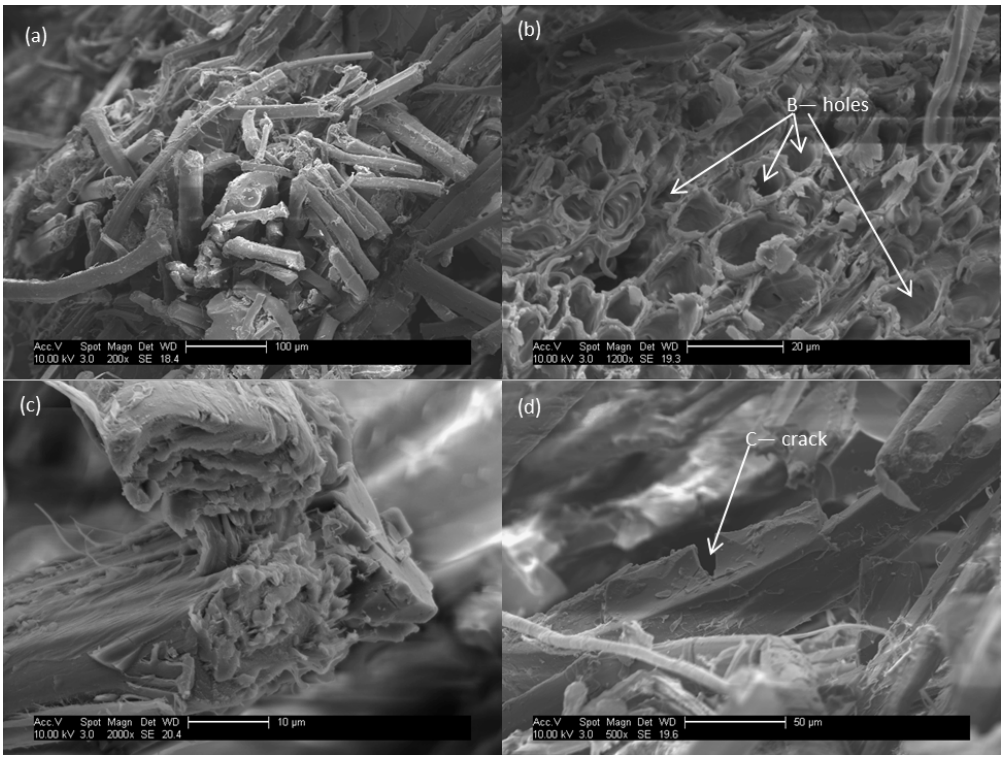

Figure 12. SEM micrographs of tensile fractured composites (Type A): (a) fracture area of composite type A; (b) holes after fibre pull-out, (c) fibre breakage, (d) brittle failure of tannin resins.

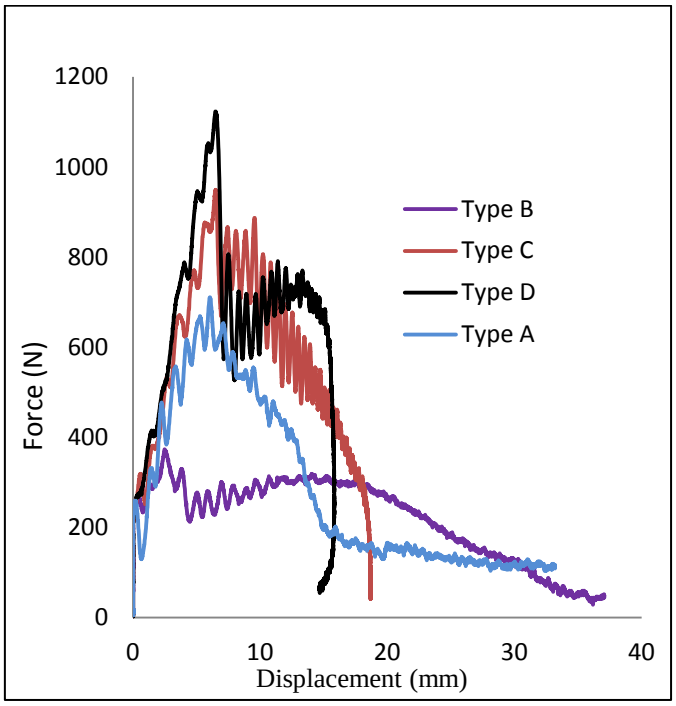

Figure 13. Force-displacement curves for different composites.

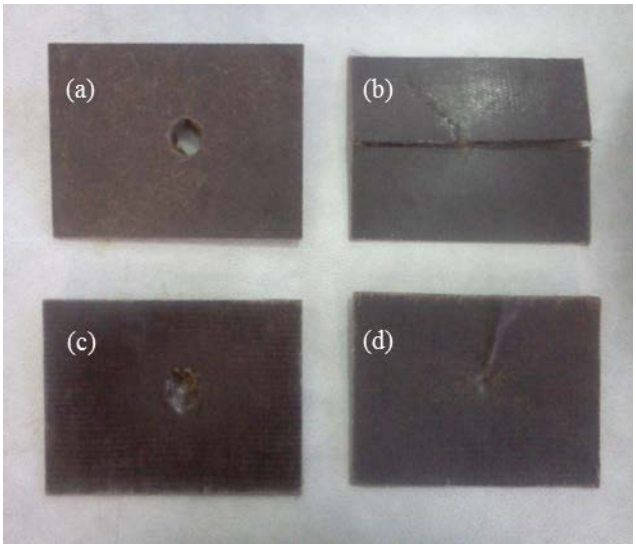

Figure 14. Examined samples after impact test: (a) Flax mat; (b) 100%UD flax (c) $[0, 90°]_4$; (d) $[0, +45°, 90°, -45°]_2$.

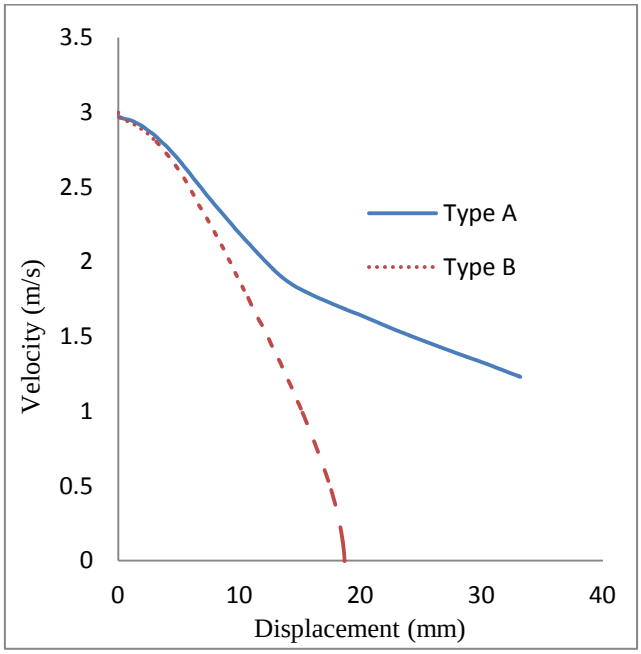

Figure 15. Velocity-displacement curves for composite A and B .

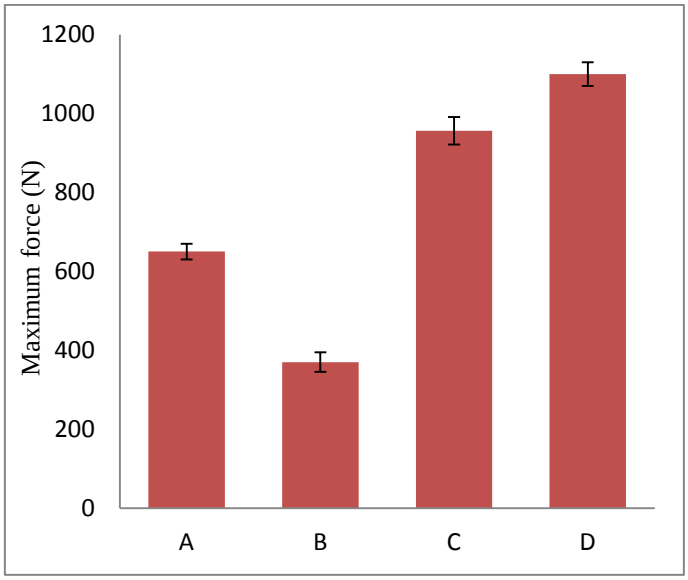

Figure 16. Maximum force for different composite types.

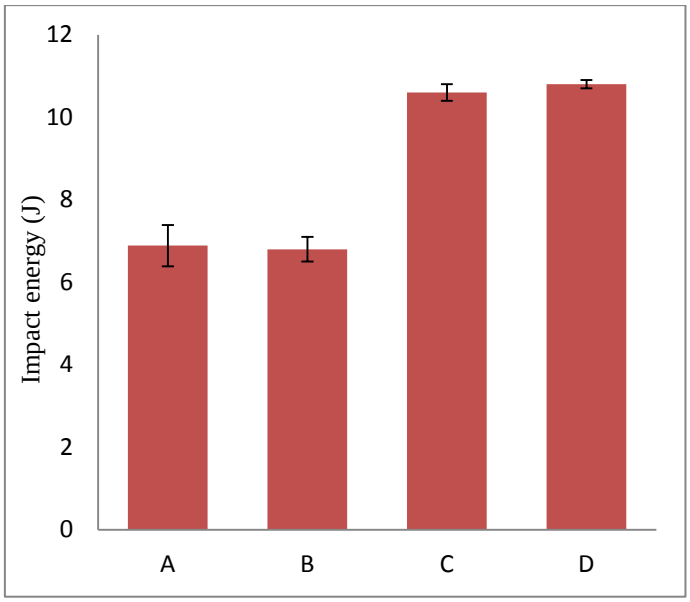

Figure 17. Impact energy for different composite types.

Tables

Table 1. Selected examples of mechanical properties of flax fibre reinforced composites.

Fibre/ Matrix	Processing	Tensile strength	Tensile modulus	Impact strength	Reference
Flax/bio-thermoset (MSO)[a]	Compression moulding	50-120 MPa	6-15 GPa		(Adekunle et al., 2012)
Flax/bio-thermoset (MMSO)[b]	Compression moulding	50-120 MPa	7-15 GPa		(Adekunle et al., 2012)
Arctic Flax/Epoxy (50:50)	Resin transfer moulding	280 MPa	40 GPa		(Oksman, 2001)
Plain woven flax/ epoxy	Hand lay-up			17-35 (kJ/m^2)	(Muralidhar et al., 2012)
Plain-woven flax/ thermoset	Compression Moulding	280 MPa	32 GPa	(Charpy) 15 kJ/m^2	(Adekunle et al., 2011)
Flax/Lactic acid resins(70:30)	Compression moulding	62 MPa	9 GPa		(Åkesson et al., 2011)
Flax/ PLA (polyactic acid)	Injection moulding	40-55 MPa	3-6 GPa	(Charpy) 9-11kJ/m^2	(Bax and Müssig, 2008)

*a-Methacrylated soybean oil, b-methacrylic anhydride-modified soybean oil.

[1]

Table 2. Investigated flax/tannin composite systems

Composite type	Fabric type	Fabric alignment	Number of layers
A	Non-woven	-	2
B	UD woven	UD (0°)	8
C	UD woven	$[0°, 90°]_4$	8
D	UD woven	$[0°, +45°, 90°, -45°]_2$	8

[2]

Table 3. Summary of DMA results of flax/tannin composites.

Composite type	E' at 27°C (GPa)	E'' at 27°C (MPa)	T_g of composite (°C)	Onset of degradation (°C)
A	5.3	194	61	150
B	7.5	516	-	160
C	6.2	345	60	-
D	5.1	379	60	158

[3]

[1] See in section 1.
[2] See in section 2.1
[3] See in section 3.1